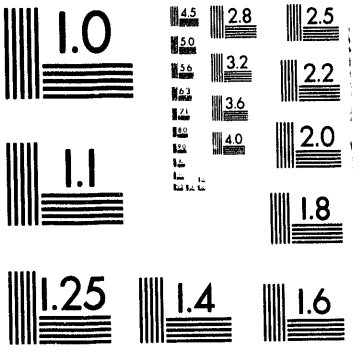
1.0
2.8
2.5
3.2
2.2
3.6
4.0
2.0
1.1
1.8
1.25
1.4
1.6

1 of 1

DOE/PC/88801--T11

IMPROVED PERFORMANCE IN COPROCESSING THROUGH FUNDAMENTAL AND MECHANISTIC STUDIES IN HYDROGEN TRANSFER AND CATALYSIS

Contract No. DE-AC22-88PC88801

Quarterly Report

June 27, 1991 - September 26, 1991

Christine W. Curtis

Department of Chemical Engineering
Auburn University, AL 36849-5127

DISCLAIMER

This report was prepared as an account of work sponsored by an agency of the United States Government. Neither the United States Government nor any agency thereof, nor any of their employees, makes any warranty, express or implied, or assumes any legal liability or responsibility for the accuracy, completeness, or usefulness of any information, apparatus, product, or process disclosed, or represents that its use would not infringe privately owned rights. Reference herein to any specific commercial product, process, or service by trade name, trademark, manufacturer, or otherwise does not necessarily constitute or imply its endorsement, recommendation, or favoring by the United States Government or any agency thereof. The views and opinions of authors expressed herein do not necessarily state or reflect those of the United States Government or any agency thereof.

MASTER

DISTRIBUTION OF THIS DOCUMENT IS UNLIMITED

IMPROVED PERFORMANCE IN COPROCESSING THROUGH FUNDAMENTAL AND MECHANISTIC STUDIES IN HYDROGEN TRANSFER AND CATALYSIS

Quarterly Report

June 27, 1991 - September 26, 1991

Submitted by

DEPARTMENT OF CHEMICAL ENGINEERING
AUBURN UNIVERSITY, ALABAMA

Dr. Christine W. Curtis, Principal Investigator

Nb45/3Q91COPROC.RPT

ACKNOWLEDGEMENTS

The experimental work of Michael Bedell, S. L. Wang and Dr. Kenneth Olson is sincerely appreciated. The technical assistance of Franklin Bowers and Joseph Aderholdt is gratefully acknowledged.

TABLE OF CONTENTS

Objective 1

Major Tasks and Their Objectives 1

Task I. Elucidation of Hydrogen Transfer Reactions in Coprocessing 1

Task II. Development of Potent Nonaromatic Hydroaromatic Donors for Coprocessing 1

Subtask I.A. Hydrogen Transfer from Cycloalkanes 1

Subtask II.E. Kinetics and Reactivity of Nonaromatic Hydroaromatic Donors 13

IMPROVED PERFORMANCE IN COPROCESSING THROUGH FUNDAMENTAL AND MECHANISTIC STUDIES IN HYDROGEN TRANSFER AND CATALYSIS

OBJECTIVE

To gain a fundamental understanding of the role and importance of hydrogen transfer reactions in thermal and catalytic coprocessing by examining possible hydrogen donation from cycloalkane/aromatic systems and by understanding the chemistry and enhanced reactivity of hydrotreated residuum, as well as by enriching petroleum solvent with potent new donors, nonaromatic hydroaromatics, thereby promoting hydrogen transfer reactions in coprocessing.

MAJOR TASKS AND THEIR OBJECTIVES

Task I. Elucidation of Hydrogen Transfer Reactions in Coprocessing

Objective. To attain fundamental understanding of the hydrogen transfer reactions which occur during coprocessing and to elucidate their role and importance in achieving upgraded products.

Task II. Development of Potent Nonaromatic Hydroaromatic Hydrogen Donors for Coprocessing

Objective. To generate petroleum solvents enriched with nonaromatic hydroaromatics by metal or electrochemical reduction and to evaluate their reactivity and selectivity.

INTRODUCTION

Research continued this quarter on Subtask I.A., Hydrogen Transfer from Cycloalkanes, and Subtask II.E. Kinetics and Reactivity of Nonaromatic Hydroaromatic Donors.

Subtask I.A. HYDROGEN TRANSFER FROM CYCLOALKANES

During this quarter, research was performed to evaluate the effectiveness of hydrogen transfer from cycloalkanes, cyclic olefins and hydroaromatic hydrogen donors to aromatic acceptor compounds. The reactions were conducted both in nitrogen and hydrogen atmospheres.

The conditions for the reactions were a reaction temperature of 380°C for 60 minutes. The reactions were performed in duplicate using small tubular microreactors that were agitated horizontally at 425 cpm. The products produced from both the hydrogen transfer agent and the aromatic species were analyzed by gas chromatography using a Varian 3300 gas chromatograph equipped with a SGE HT-5 fused silica column and FID detection. Products were identified by comparison of retention times with authentic compounds and by GC-mass spectral analysis using a VG 70EHF mass spectrometer. Quantitative analysis was achieved by using the internal standard method with biphenyl as the internal standard. The GC analysis of each reaction was duplicated. The results are presented as averages with standard deviations of the product distributions from the reactions. The reactions performed during this quarter served as the ground work for catalytic reactions to be performed next quarter using a sulfur containing organic compound as the catalyst.

Reactions with Anthracene. Reactions were conducted in which the hydrogen-rich species, tetralin (TET) and perhydropyrene (PHP), were reacted with anthracene (ANT). In addition, reactions of the individual pure compound, both hydrogen donors and acceptors, were also performed to ascertain the effect of the reaction temperature and atmosphere on their reactivity.

The product distributions from the reactions of TET and ANT in N_2 and H_2 atmospheres are given in Table 1. TET did not react in either atmosphere while ANT hydrogenated to form dihydroanthracene (DHA) in H_2 but was not reactive in N_2. Reactions of the combined systems showed that in a system containing 1 to 1 ratio of TET to ANT, TET had no reactivity; however, more hydrogenation of ANT to DHA occurred in the presence of H_2 with TET than

without TET. Also, a trace amount of tetrahydroanthracene (THA) was also formed. The same phenomenon occurred at the 5 to 1 ratio of TET to ANT in both H_2 and N_2 atmospheres compared to the individual compound reactions. An increase in the amount of DHA formed occurred in the reaction with N_2 with a 5 to 1 ratio of TET to ANT.

This increase is also observed in Table 6 which gives the percent hydrogenation (% HYD) of aromatics from reactions involving aromatics and hydrogen-rich species. The percent hydrogenation is defined as the number of moles of H_2 required to achieve the final product as a percentage of the number of moles required to form the most hydrogenated product. The % HYD of ANT increased from 0.25% in the 1 to 1 TET/ANT system to 2.64 in the 5 to 1 TET/ANT system. Calculation of the moles of hydrogen released during the reaction given in Table 7 showed that a small amount of hydrogen was released in the 5 to 1 TET to ANT in both H_2 and N_2 atmospheres.

Reactions of perhydropyrene (PHP) with ANT showed a substantial effect of atmosphere on the hydrogenation of ANT to DHA. In a hydrogen atmosphere at both 1 to 1 and 5 to 1 ratios of PHP to ANT, 12.3 and 15.9 mole % DHA was formed. When ANT was reacted individually nearly 12% DHA was formed so that substantial hydrogenation of ANT occurred in the presence of molecular H_2. Almost no DHA was formed in the reaction of ANT individually in a N_2 atmosphere. With PHP present in N_2, 1.8% and 2.5% DHA were formed in the 1 to 1 and 5 to 1 PHP to ANT reactions, respectively. Detectable amounts of pyrene (PYR) were observed in both atmospheres at both reactant ratios. The most dehydrogenation of PHP occurred in the reaction with N_2 at a 5 to 1 ratio of PHP to ANT. The % HYD of ANT

was nearly equivalent for each atmosphere regardless of the ratio of cycloalkanes to aromatic. The most moles of H_2 were released in a N_2 atmosphere with a 5 to 1 ratio of PHP to ANT.

Reactions with Pyrene. Pyrene was used as the hydrogen acceptor in several systems. The hydrogen donors used were TET, hexahydroanthracene (HHA) and DHA. The reaction of TET with PYR showed little reactivity regardless of atmosphere or ratio of donor to acceptor. However, in the 5 to 1 TET to PYR system, more reactivity was observed in terms of PYR forming DHP. These results were reflected in the % HYD given in Table 6 where the most HYD was observed in the 5 to 1 ratio experiments.

HHA was extremely reactive under these reactions conditions employed. After 60 minutes of reaction, nearly all of the HHA reacted leaving slightly more than 4 mole % as HHA. The compounds present at the end of the reaction included ANT, DHA, THA, HHA, and octahydroanthracene (OHA). No reactivity occurred in the PYR system when PYR was introduced alone; however, in the presence of HHA, three products were formed DHP, tetrahydropyrene (THP) and hexahydropyrene (HHP).

Substantial reactivity of PYR was observed. In a 1 to 1 HHA to PYR reaction system, more than 33% conversion of PYR occurred in H_2 while ~20% conversion occurred in N_2. The primary product formed was DHA although measurable amounts, though small, were observed of THP and HHP. In the corresponding product slates from HHA, DHA was the primary product with THA and ANT being the secondary products in nearly equivalent amounts.

The reactions containing a 5 to 1 HHA to PYR showed substantial differences in their reactivities in the two atmospheres of H_2 and N_2. Nearly 60% conversion of PYR occurred in the H_2 reaction with DHP being the primary product but with substantial amounts of THP and

HHP being formed. In N_2, much less conversion of PYR occurred with DHP and HHP being the primary products. HHA also showed a different product slate between the N_2 and the H_2 atmospheres. Much more ANT was formed in the N_2 system than the H_2 while much more DHA was formed in H_2 than N_2, indicating that the H_2 atmosphere slowed the dehydrogenation of the hydrogenated anthracene products.

The amount of hydrogenation of the aromatic PYR occurring in the HHA/PYR system was substantial. In H_2, 13.6% and 30.4% HYD occurred in the 1 to 1 and 5 to 1 systems, respectively. By contrast, the amount of hydrogenation in the N_2 system was 8.1 and 10.4%, respectively. Obviously, the H_2 atmosphere had a direct effect on the amount of hydrogenation. The moles of H_2 released were very similar in the 1 to 1 HHA to PYR system in both N_2 and H_2 atmosphere. Hence, the H_2 atmosphere directly influenced the hydrogenation of the PYR in the presence of a donor but did not when no donor was present.

DHA reacted to a much lesser extent individually and with PYR than did HHA. Individually, ~7% conversion of DHA occurred in H_2 and ~5% with N_2 with PYR present, ~10% DHA conversion occurred regardless of atmosphere and ratio of donor to acceptor. The primary product was ANT for all the reactions with a very small amount of THA being formed.

Substantial differences were observed in PYR conversion between the reactions having a 1 to 1 and a 5 to 1 DHA to PYR ratio. Conversions of ~5 to 7% were observed in the 1 to 1 DHA to PYR reactions with the primary product being DHP. Substantially, more conversion of ~20% was obtained at the higher ratio with DHP being the primary product and HHP the secondary.

The % HYD of PYR showed substantial increases at the higher ratio compared to the lower ratio for both atmospheres. The number of moles of hydrogen released was 3 to 4 times at the 5 to 1 ratio compared to the 1 to 1 ratio.

SUMMARY

The reactions with cyclic olefin HHA showed substantial reactivity both in conversion of HHA and in the hydrogenation of PYR. The presence of H_2 strongly influenced the amount of hydrogenation obtained. The hydrogen donor DHA resulted in substantial hydrogenation of PYR but was strongly influenced by the ratio of DHA to PYR. The cycloalkane PHP showed some hydrogen transfer forming small amounts of PYR. ANT hydrogenation was affected substantially by the molecular hydrogen present which responsible for most of the hydrogenation, although a small amount of the hydrogenation occurred through hydrogen transfer from the cycloalkane. TET was essentially nonreactive.

Future work will consist of reacting isotetralin with these various acceptors as well as performing catalytic reactions using an organic sulfur compound as the catalyst.

Table 1. Product Distributions for Reactions of Tetralin with Anthracene

	Product Distributions, mole %				
	From Tetralin		From Anthracene		
	TET	NAP	ANT	DHA	THA
Tetralin					
H_2	99.64±0.09	0.36±0.10			
N_2	99.78±0.02	0.22±0.02			
Anthracene					
H_2			88.31±1.07	11.68±1.06	0±0
N_2			99.53±0.76	0.47±0.16	0±0
TET/ANT (1:1)					
H_2	99.62±0.03	0.38±0.04	82.11±1.05	17.64±1.02	0.25±0.03
N_2	99.93±0.08	0.06±0.07	98.96±0.22	1.04±0.22	0±0
TET/ANT (5:1)					
H_2	99.84±0.04	0.16±0.04	82.75±0.84	16.66±0.71	0.57±0.21
N_2	99.20±0.53	0.55±0.04	89.40±0.61	10.59±0.61	0±0

TET = tetralin
NAP = naphthalene
ANT = anthracene
DHA = dihydroanthracene
THA = tetrahydroanthracene

Table 2. Product Distributions for Reactions of Perhydropyrene with Anthracene

	Product Distributions, mole %			
	From Perhydropyrene		From Anthracene	
	PHP	PYR	ANT	DHA
PHP				
H_2	100±0	0±0		
N_2	100±0	0±0		
ANT				
H_2			88.3±1.07	11.7 ±1.06
N_2			99.5±0.76	0.47±0.16
PHP/ANT (1:1)				
H_2	99.3±0.07	0.74±0.08	87.7±1.11	12.3 ±1.10
N_2	99.2±0.13	0.78±0.14	98.2±0.66	1.82±0.67
PHP/ANT (5:1)				
H_2	99.9±0.01	0.10±0.01	84.0±1.59	15.9 ±1.67
N_2	98.6±0.17	1.38±0.18	97.5±0.08	2.53±0.08

PHP = perhydropyrene
PYR = pyrene
ANT = anthracene
DHA = dihydroanthracene

Table 3. Product Distributions for Reactions of Tetralin with Pyrene

	Product Distributions, mole %			
	From Tetralin		From Pyrene	
	TET	NAP	PYR	DHP
TET				
H_2	99.64±0.09	0.36±0.10		
N_2	99.78±0.02	0.22±0.02		
PYR				
H_2			100±0	0±0
N_2			100±0	0±0
TET/PYR (1:1)				
H_2	100±0	0±0	100±0	0±0
N_2	100±0	0±0	100±0	0±0
TET/PYR (5:1)				
H_2	99.89±0.01	0.11±0.00	98.76±0.30	1.24±0.29
N_2	99.61±0.25	0.39±0.25	99.33±0.04	0.68±0.04

TET = tetralin
NAP = naphthalene
PYR = pyrene
DHP = dihydropyrene

Table 4. Product Distributions for Reactions of Hexahydroanthracene with Pyrene

	Product Distributions, mole %								
	From Hexahydroanthracene					From Pyrene			
	ANT	DHA	THA	HHA	OHA	PYR	DHP	THP	HHP
HHA									
H_2	5.08±1.49	80.88±0.58	8.03±0.44	4.41±0.66	1.58±0.89				
N_2	7.40±0.39	77.80±1.03	8.46±0.66	4.19±0.33	2.05±0.25				
PYR									
H_2						100±0	0±0	0±0	0±0
N_2						100±0	0±0	0±0	0±0
HHA/PYR (1:1)									
H_2	7.08±0.19	76.08±0.19	11.81±0.58	2.97±0.24	2.04±0.23	66.57±0.51	28.49±0.55	2.49±0.20	2.44±0.13
N_2	18.46±0.89	50.46±3.10	23.28±2.75	3.77±0.19	4.01±0.71	79.14±2.29	18.73±1.79	0.64±0.74	1.48±0.24
HHA/PYR (5:1)									
H_2	4.68±0.29	51.41±0.97	24.99±0.28	9.23±0.45	9.68±0.31	40.67±1.95	39.29±1.52	8.30±0.45	11.72±0.44
N_2	26.15±2.54	25.10±2.68	38.18±0.48	4.72±0.08	5.83±0.36	83.70±1.66	8.81±1.50	0.0 ±0.0	7.48±2.93

ANT = anthracene
DHA = dihydroanthracene
THA = tetrahydroanthracene
OHA = octahydroanthracene

PYR = pyrene
DHP = dihydropyrene
THP = tetrahydropyrene
HHP = hexahydropyrene

Table 5. Product Distributions for Reactions of Dihydroanthracene and Pyrene

	Product Distributions, mole %						
	From Dihydroanthracene			From Pyrene			
	ANT	DHA	THA	PYR	DHP	THP	HHP
DHA							
H_2	6.86±0.67	92.78±0.45	0.34±0.49				
N_2	5.30±0.20	94.69±0.20	0.0 ±0.0				
PYR							
H_2				100±0	0±0	0±0	0±0
N_2				100±0	0±0	0±0	0±0
DHA/PYR (1:1)							
H_2	8.69±0.12	90.61±0.40	0.70±0.30	93.61±0.82	5.73±1.57	0.0 ±0.0	0.65±0.75
N_2	9.63±1.00	90.19±1.13	0.17±0.20	95.36±2.17	4.64±2.17	0.0 ±0.0	0.0 ±0.0
DHA/PYR (5:1)							
H_2	8.33±0.16	90.46±0.19	1.19±0.06	78.48±0.07	15.10±0.47	0.49±0.04	5.92±0.52
N_2	7.77±0.74	91.11±0.94	1.10±0.20	81.91±2.30	14.08±0.26	0.20±0.23	3.77±2.08

ANT = anthracene
DHA = dihydroanthracene
THA = tetrahydroanthracene

PYR = pyrene
DHP = dihydropyrene
THP = tetrahydropyrene
HHP = hexahydropyrene

Table 6. Percent Hydrogenation of Aromatics from Reactions Involving Aromatics and Hydrogen-Rich Species

Reaction System	Atmosphere H_2	Atmosphere N_2
	% HYD	% HYD
HHA/PYR (1:1)	13.59(0.23)	8.14(0.84)
HHA/PYR (5:1)	30.35(0.97)	10.40(2.48)
DHA/PYR (1:1)	2.46(0.18)	1.63(0.85)
DHA/PYR (5:1)	11.27(0.35)	8.58(2.17)
TET/ANT (1:1)	4.53(0.26)	0.25(0.05)
TET/ANT (5:1)	4.45(0.25)	2.64(0.15)
TET/PYR (1:1)	0.00(0.00)	0.00(0.00)
TET/PYR (5:1)	0.41(0.09)	0.16(0.01)
PHP/ANT (1:1)	3.07(0.27)	0.45(0.17)
PHP/ANT (5:1)	3.97(0.41)	0.60(0.04)

% HYD = percent hydrogenation

For the calculation of %HYD, the most hydrogenated liquid product for pyrene was hexahydropyrene and for anthrancene was octahydroanthracene.

Table 7. Net Moles of H_2 Released During Reaction

Reaction System	Atmosphere H_2 Moles x10^4	Atmosphere N_2 Moles x10^4
HHA	9.95±0.31	9.95±0.09
HHA/PYR (1:1)	9.93±0.01	9.52±0.31
HHA/PYR (5:1)	35.84±0.48	43.67±0.82
DHA	0.35±0.06	0.28±0.0
DHA/PYR (1:1)	0.43±0.01	0.52±0.05
DHA/PYR (5:1)	1.96±0.03	1.78±0.19
TET	0.05±0.03	0.03±0.0
TET/ANT (1:1)	0.05±0.02	0.0 ±0.0
TET/ANT (5:1)	0.11±0.03	0.41±0.03
TET/PYR (1:1)	0.0 ±0.0	0.0 ±0.0
TET/PYR (5:1)	0.0 ±0.0	0.28±0.19
PHP	0.0 ±0.0	0.0 ±0.0
PHP/ANT (1:1)	0.26±0.02	0.28±0.05
PHP/ANT (5:1)	0.18±0.01	2.52±0.31

Subtask II.E. KINETICS AND REACTIVITY OF NONAROMATIC HYDROAROMATIC DONORS

Work this quarter consisted of the investigation into the catalytic reactivity of the cyclic olefins, isotetralin (ISO) and hexahydroanthracene (HHA), to compare their reactivity to that of their conventional donor analogues tetralin (TET), octahydroanthracene (OHA), and dihydroanthracene (DHA). The catalysts used were presulfided, pulverized $NiMo/Al_2O_3$ and Mo/Al_2O_3. Once the experimental reactivity and product slates were determined for the model compounds, pseudo first order reaction rate constants, Arrhenius parameters and Gibbs free energy values were determined for the catalytic reactions. This work is a continuation of the results for the thermal reactivity presented last quarter.

EXPERIMENTAL PROCEDURE

Reaction Procedures. The reactivity of the cyclic olefins and their conventional hydrogen donor analogues was tested in stainless steel tubing bomb reactions with volumes of 20 cm^3 under the following conditions: 380°C, horizontal agitation at 425 cpm, 1250 psig nitrogen or hydrogen pressure at ambient temperature, reaction times ranging from 2 minutes to 1 hour, 2.0g hexadecane as the diluent solvent, reaction mixtures containing 3 weight percent hydrogen donor, and a total active metal loading of 3000 ppm. Two catalysts were used, Shell 324, $NiMo/Al_2O_3$, and Amocat 1B, Mo/Al_2O_3, to evaluate the catalytic reactivity of the hydrogen donors at liquefaction conditions. Each catalyst was presulfided in a heated flowing stream of 10% H_2S in H_2 for approximately five hours, pulverized, and sized between 100 and 200 mesh before being used. The catalyst was stored in a desiccator until they were used.

The chemicals used in this study were obtained from the following manufacturers and used as received: tetralin, 1,4,5,8,9,10-hexahydroanthracene, 1,2,3,4,5,6,7,8-octahydroanthracene, 9,10-dihydroanthracene, hexadecane from Aldrich Chemical Co.; 1,4,5,8-tetrahydronaphthracene from Wiley Organics Inc.

The products from the model reactivity studies were analyzed by gas chromatography using a Varian 3400 gas chromatograph equipped with a HT-5 column from SGE and FID detection. The internal standard method was for quantitation, with biphenyl as the internal standard. The peaks were identified by comparing retention times with authentic compounds and by GC mass spectral analysis using a VG 70EHF mass spectrometer.

BACKGROUND AND THEORY

For the thermal dehydrogenation reactions of the cyclic olefins and their conventional hydrogen donor compound, it was assumed that the reaction kinetics could be approximated by a pseudo-first-order rate expression (1). The overall reaction was expressed as A --> products, where A was ISO, TET, DHA, HHA, or OHA. On the basis of the first order kinetics and defining C as the concentration of the reactant A, the rate law as expresses as

$$rate\ -dC/dt = kC \tag{1}$$

separation of variables and integration of (1) yielded

$$\int_{Co}^{C} dC/C = -k \int_{o}^{t} dt \tag{2}$$

where C_o is the initial concentration of reactant A, k is the apparent rate constant, t is the time of the reaction and C is the concentration of reactant A at the time t, and therefore

$$\ln C_o/C = kt \tag{3}$$

In the analysis of the experimental reactions, the weight percent of the reactant was determined at discrete reaction times ranging from 2 minutes to 120 minutes, as necessary. The weight percent remaining of reactant A at time t was defined as λ and was proportional to the concentration of the reactant. Assuming that λ varied in a linear fashion with the extent of reaction, the concentration of A can be defined as

$$C(t) = p\ (\lambda - \lambda_\infty) \tag{4}$$

where λ_∞ is the value of the weight percent of A at the end of the reaction, e.g. as t --> ∞, $\lambda = 0$ and p is a proportionality constant. Using the additional boundary condition that at t = 0, $\lambda = 100$, i.e. no reaction has initially occurred, then

$$C_o = p(\lambda_o - \lambda_\infty) \tag{5}$$

and substitution of equations (4) and (5) into equation (3) yields

$$\ln \{(\lambda_o - \lambda_\infty)\ /\ (\lambda - \lambda_\infty)\} = kt \tag{6}$$

however, $\lambda_o = 100$, and $\lambda_\infty = 0$, therefore, equation (6) becomes

$$\ln\ (\lambda_o\ /\ \lambda) = kt \tag{7}$$

which upon manipulation and rearrangement becomes

$$\lambda = 100\ e^{(-kt)} \tag{8}$$

and the linear form of equation (8) becomes

$$\lambda = -kt + \ln(100) \tag{9}$$

Therefore, a plot of ln λ versus t should yield a straight line. The slope of the line obtained is the apparent rate constant, k, for the reaction at a given temperature. For the experimental results obtained, the ln λ versus t data was analyzed via linear regression to obtain the best fit and subsequent value for k.

Once the apparent rate constant was determined at three different temperatures for each of the five model compounds, the next step was to investigate the effect of temperature on the rate constants. This step was accomplished by using the Arrhenius equation,

$$\ln k = \ln k_o - E_a/RT \tag{10}$$

where E_a is the activation energy, k_o is the frequency factor, T is the temperature, and R is the universal gas constant. The magnitude of the activation energy is an indication of the temperature sensitivity of a given reaction. The frequency factor accounts for other effects, e.g. frequently of collisions, geometric constraints, etc., that influence the rate of reaction. Reactions with large values of E_a are temperature sensitive, while those reactions with a small value of E_a are relatively unaffected by changes in temperature. Using equation (10), E_a and k_o, yielded the following equations for a gas phase, unimolecular reaction, e.g. A--> products:

$$E_a = \Delta H + RT \tag{11}$$

and

$$k_o = \{(e\ k_b\ T)/h\}\ e^{\Delta S/R} \tag{12}$$

where k_b is the Boltzman constant, h is Plank's constant, ΔH is the entropy, ΔS in the entropy and e = 2.718. Equation (13) can be used to determine the Gibbs free energy of formation as a function of temperature.

$$\Delta G = \Delta H - T\,\Delta S \tag{13}$$

In order to use equation (13), equations (11) and (12) must be rearranged to obtain $\Delta H = f(E_a,T)$ and $\Delta S = f(k_o,T)$. These relations become

$$\Delta H = E_a - RT \tag{14}$$

and

$$\Delta S = R \ln (k_o/T) + R\beta \tag{15}$$

where β is a constant and is equal to $\ln \{h / (e\, k_b)\}$. Substitution of equations (14) and (15) into equation (13) yields

$$\Delta G = E_a - RT(1+\beta) - RT \ln(k_o/T) \tag{16}$$

which provides $\Delta G = f(E_a,k_o,T)$. For a given compound, with the corresponding values of E_a and k_o, a relationship for the Gibbs free energy as a function of temperature can be developed. The value for ΔG can be used to form a basis for comparing the reactivities of the model compounds. The more negative the value for ΔG, the more spontaneous the reaction will proceed, i.e. the more reactive the compound.

CATALYTIC REACTION PRODUCT SLATES

The catalytic reactions of the cyclic olefins and their conventional hydrogen donor analogues were performed with a commercial $NiMo/Al_2O_3$ catalysts (Shell 324) and a Mo/Al_2O_3 catalyst (Amocat 1b) at various reaction times and three different temperatures. Table 8 through 17 present the results that were obtained in these catalytic reactions. There were up to five

reaction times, including $\lambda = 0$ at $t = 0$, used to fit the experimental data to the pseudo first order kinetics model.

Reactions with ISO and the Mo/Al_2O_3 catalyst were performed at 225, 175, and 125°C as given in Table 8. At 225°C, the primary reaction products from ISO were TET and OHN, with lesser amounts of 1,4- and 1,2-DHN. At 175°C, the primary reaction products were 1,4-DHN and TET. At 125°C, 1,4-DHN was the predominant reaction product with a minor amount of TET and 1,2-DHN also being formed. The results of the reactions with ISO at 175, 140, and 100°C with the $NiMo/Al_2O_3$ catalyst are given in Table 9. At 175°C, 1,4-DHN, TET, and OHN were the primary reaction products with a small amount of 1,2-DHN also being produced. The same products were obtained in the reactions at 140°C, with TET being the major product At 100°C, 1,4-DHN was the only product formed. At reaction temperatures of 380, 425, and 450°C, as shown in Table 10, 1,2-DHN, t-DEC, and a minor amount of NAP were produced in the reactions of TET with the Mo/Al_2O_3 catalyst, with the addition of c-DEC, at 380, 425, and 450°C (Table 11).

OHA, THA, and ANT were the only reaction products from DHA in reactions with the Mo/Al_2O_3 catalyst at 380, 350, and 300°C as shown in Table 12. In addition to OHA, THA, and ANT, PHA was produced from DHA in reactions with the $NiMo/Al_2O_3$ catalyst at the same reaction temperatures (Table 13). Reactions with OHA and the Mo/Al_2O_3 catalyst were performed at 450, 425, and 380°C (Table 14). The primary reaction product was THA at 450°C, with a lesser amount of THA also formed. At the lower reaction temperatures of 380, 425, and 450°C (Table 15), PHA was the primary reaction product from OHA in reactions with the $NiMo/Al_2O_3$ catalyst. THA, DHA, and ANT were also produced in lesser amounts. At

reaction temperatures of 225 and 175°C (Table 16), HHA was primarily converted to OHA in reactions with the Mo/Al_2O_3 catalyst; lesser amounts of THA and PHA were also produced. At 125°C, nearly equivalent amounts of OHA and THA were produced. Reactions were performed with HHA and the $NiMo/Al_2O_3$ catalyst at 175, 140, and 100°C (Table 17). OHA was the primary reaction product, with lesser amounts of THA and DHA also being formed.

In examining the data from Table 8 through 17, the cyclic olefins were much more reactive catalytically than their conventional hydrogen donor analogues. ISO and HHA required much lower temperatures to be reactive when compared to their conventional hydrogen donor analogues, less than 225°C compared to 450°C. The cyclic olefins also required much shorter reaction times to be converted. This high degree of reactivity of the cyclic olefins was also observed in thermal reaction systems discussed in the first part of this chapter.

KINETIC ANALYSIS AND ARRHENIUS PLOTS FOR THE CATALYTIC REACTION OF THE COMPOUNDS UNDER NITROGEN AND HYDROGEN

Using equation (9) and the data presented in Tables 8 through 17, the apparent rate constant k and linear regression correlation coefficients were determined for the reactions of the model compounds at a particular reaction temperature in the reactions of both the $NiMo/Al_2O_3$ and Mo/Al_2O_3 catalysts. The results that were obtained are summarized in Table 18. As can be seen, the fit of the experimental data to the pseudo-first order reaction kinetic model was good for the reactions with both $NiMo/Al_2O_3$ and Mo/Al_2O_3 catalysts. The straight line correlation coefficients, r, were 0.92 or greater and were usually greater than 0.95. For all of the compound studied, with both catalysts, the rate constants increased with an increase in

reaction temperature, i.e. a higher reaction temperature increased the rate of reaction for all the model compounds.

At reaction temperatures greater than ~225°C, the cyclic olefins reacted so rapidly that no kinetic data could be obtained. By contrast, the conventional donors were unreactive at these lower temperatures. Because there was no common reaction temperature between the cyclic olefins and their analogues, no direct comparison of rate constants can be made.

With the reactions of HHA and ISO with Mo/Al_2O_3 at 225°C, the rate constant for ISO was 2 times that for HHA. At 175°C, the rate constant for ISO was 3.2 times greater than that of HHA, while at 125°C, the rate constant for HHA was 1.9 times that of ISO. With the reactions of $NiMO/Al_2O_3$ with HHA and ISO, at 175°C and 100°C the rate constant for HHA was greater than that for ISO, while at 140°C the rate constant for ISO was larger.

The three conventional hydrogen donor compounds had a common reaction temperature of 380°C with both catalysts. With the reactions of the Mo/Al_2O_3 catalyst, the rate constant for DHA was 35.9 times greater than that obtained for TET, and 27.1 times greater than that of OHA. With the $NiMo/Al_2O_3$ catalyst, the rate constant for TET was nearly equivalent to that of OHA and slightly less than that of DHA.

Using the data in Table 18 for the apparent rate constants and equation (10), Arrhenius plots were developed for the five model compounds in reactions with both $NiMo/Al_2O_3$ and Mo/Al_2O_3. From the linear regression of this data, values for Ea and K_o were obtained. These values are summarized in the last column of Table 18. The fit of the Arrhenius plots to the experimental data was, in general, good as evidenced by the straight line correlation coefficients being 0.97 or greater. However, there are three notable exceptions, the reactions of DHA and

OHA with the $NiMo/Al_2O_3$ catalyst and the reaction of HHA with the Mo/Al_2O_3 catalyst. The coefficients for these reactions ranged from ~0.85 to ~0.90. The poor fit of the Arrhenius plots to these reactions was believed to be caused by experimental fluctuations, rather than a change in the effect of temperature on the activation energy. Additional reactions should be performed to investigate this matter further. To develop the Gibbs free energy plots for the catalytic reactions, the best fit to the experimental data was obtained and the corresponding values for Ea and k_o determined.

For the reactions of the model compounds with the Mo/Al_2O_3 catalyst, the activation energy shows the following trend: TET > DHA > OHA > ISO > HHA. For the reactions with the $NiMo/Al_2O_3$ catalyst, the activation energy shows the following trend: DHA > HHA > ISO > TET > OHA.

DETERMINATION OF GIBBS FREE ENERGY FOR THE CATALYTIC REACTIONS

Using the Arrhenius parameters for a given model compounds in the catalytic reaction system and equation (16), plots of the Gibbs free energy versus temperature were developed. Figures 1 and 2 present the noncatalytic reaction results. Figure 3 presents the results that were obtained for the reactions with the Mo/Al_2O_3 catalyst, while Figure 4 presents the corresponding results for the reactions with the $NiMo/Al_2O_3$ catalyst.

As was the case in the thermal reaction systems, under both nitrogen and hydrogen, the more dramatic feature of the results for the Gibbs free energy plots with the Mo/Al_2O_3 catalyst was the fact that the cyclic olefins have much lower (more negative) values for ΔG. This result implies that their reactions should be more spontaneous than their conventional hydrogen donor analogues. Experimentally, the cyclic olefins were indeed more reactive.

At temperatures of 125, 175, and 225°F, Figure 1 suggests that the reactions of ISO should be favored because of its lower values for ΔG than those for HHA. When Tables 8, for ISO, and 16, for HHA, are compared, experimentally ISO was converted more than HHA at a given reaction time.

At 380°C, a common reaction temperature for the three conventional donors, the reactivity ranking, as determined by the magnitude of the Gibbs free energy, should be that DHA was much more reactive than either OHA of TET. OHA and TET should also have had nearly equivalent levels of reactivity. Experimentally, DHA was converted 93.7% in 60 minutes, while OHA was converted 9.5% and TET converted 7.2%. The experimental results are in excellent agreement with those predicted by the relative values of the Gibbs free energy.

As was the case with the Mo/Al_2O_3 catalyst, for the reactions with $NiMo/Al_2O_3$, the cyclic olefins ISO and HHA had much lower values for the Gibbs free energy than TET, OHA and DHA. Experimentally, they also required much lower temperatures and shortened reaction times to be converted.

The plots in Figure 4 suggest that ISO and HHA should have very similar levels or reactivities, by the overlap of their respective plots. This result was substantiated by the results for the conversion of ISO and HHA at 175°C. With a reaction time of 2 minutes, ISO was converted 47.5% and HHA was converted 44.2%; with a reaction time of 5 minutes, ISO was converted 81.9% and HHA was converted 77.6%; with a reaction time of 7 minutes, ISO was converted 91.6% and HHA was converted 95.2%. The experimental reactivity of ISO and HHA were nearly equivalent, as was predicted by the Gibbs free energy values.

At 380°C, a common reaction temperature for OHA, DHA, and TET, from Figure 4, DHA should be much more reactive than TET or OHA. TET and OHA should have very similar reactivities. In a reaction time of 2 minutes, DHA was converted 13.2%, TET 3.2% and OHA 17.2%. The prediction by the Gibbs free energy correctly described the experimental results for DHA and TET, yet underestimated the reactivity of OHA. However, for the reactions of OHA and DHA, as was previously discussed, there was more experimental deviations and the correlation coefficients for the Arrhenius plots were only 9.85 for DHA and 0.88 for OHA. The variability of the experimental results for the reactions may limit the accuracy of the Gibbs free energy plots based upon the calculated values for Ea and k_o. However, regardless of the slight variations in the ranking of the conventional donor compounds reactivity, the trends that the cyclic olefins were much more reactive than OHA, DHA, or TET was substantiated by their much lower values for the Gibbs free energy of reaction. The magnitudes of the differences between the CLO's and their analogues were great enough to be outside the influence of experimental variations.

CONCLUSIONS

The reactions of ISO, HHA, TET, OHA and DHA were performed with $NiMo/Al_2O_3$ and Mo/Al_2O_3 catalyst at reaction temperatures ranging from 100 to 450°C and reaction times from 2 to 90 minutes. Both ISO and HHA were essentially completely converted at 225°C with the Mo/Al_2O_3 catalyst and a reaction time of 15 minutes. In contrast, DHA and TET required 450°C and a reaction of 60 minutes to be converted ~90%; OHA was ~70% converted at 450°C and 60 minutes.

ISO and HHA were almost completely converted at 170°C and a reaction time of 7 minutes, whereas OHA and TET required a reaction temperature of 450°C and a reaction time of 60 minutes to show similar levels of conversion. At 175 and 225°C, with the Mo/Al_2O_3 catalyst, the apparent rate constant of ISO was greater than that of HHA, while at 125°C, that of HHA was larger than that of ISO. With the reactions of the $NiMo/Al_2O_3$ catalyst with HHA and ISO, at 100 and 175°C the rate constant for HHA was greater than that for ISO, while at 140°C the rate constant for ISO was larger.

For the plots of ΔG versus T for the reactions with both catalyst, the cyclic olefins had much lower values for ΔG than OHA, DHA and TET. Therefore, the cyclic olefins, from a thermodynamic standpoint, should be more reactive than their conventional donor analogues, which was well supported by experimental evidence.

Both the kinetic data via the reaction rate constants, and the thermodynamic results, that is, the values for the Gibbs free energy, predicted that the cyclic olefins should be more reactive than their conventional hydrogen donor analogues. Experimentally, ISO and HHA were found to be much more reactive than TET, OHA and DHA.

NOMENCLATURE

ANT	=	anthracene	HHN	=	hexahydronaphthalene
c-DEC	=	cis-decalin	ISO	=	isotetralin
t-DEC	=	trans-decalin	NAP	=	naphthalene
DHA	=	dihydroanthracene	OHA	=	octahydroanthracene
DH	=	donable hydrogen	OHN	=	octahydronaphthalene
1,2-DHN	=	1,2-dihydronaphthalene	PHA	=	perhydroanthracene
1,4-DHN	=	1,4-dihydronaphthalene	TET	=	tetralin
HHA	=	hexahydroanthracene	THA	=	tetrahydroanthracene

Table 8. Products from the Reaction of Isotetralin with Mo/Al_2O_3

Reaction Conditions	Weight Percent Recovered				
	OHN	TET	1,2-DHN	1,4-DHN	ISO
ISOTETRALIN					
225°C					
2 MIN	9.4(0.4)	45.0(1.6)	8.1(0.1)	11.2(0.3)	23.9(2.1)
5 MIN	19.3(0.2)	64.2(0.1)	6.7(0.3)	4.0(1.4)	5.7(0.1)
10 MIN	22.7(0.1)	77.3(0.1)	0.0	0.0	0.0
15 MIN	20.9(0.5)	79.1(0.5)	0.0	0.0	0.0
175°C					
2 MIN	0.0	3.4(0.2)	1.8(0.2)	14.6(0.8)	80.3(1.03)
15 MIN	0.7(0.8)	7.7(4.7)	5.7(3.8)	25.1(14.75)	60.8(6.2)
30 MIN	5.6(1.2)	33.3(1.4)	8.1(1.1)	29.3(3.5)	23.4(2.0)
125°C					
2 MIN	0.0	0.0	0.0	6.7(0.9)	93.3(0.9)
15 MIN	0.0	0.0	0.9(0.1)	10.9(0.2)	88.3(0.2)
30 MIN	0.0	1.6(0.3)	1.5(0.1)	10.8(1.0)	86.0(1.5)
60 MIN	0.0	7.4(0.2)	7.0(0.4)	11.0(0.5)	74.6(1.1)

Table 9. Products from the Reaction of Isotetralin with $NiMo/Al_2O_3$

Reaction Conditions	Weight Percent Recovered				
	OHN	TET	1,2-DHN	1,4-DHN	ISO
ISOTETRALIN					
175°C					
2 MIN	2.6(3.0)	12.3(5.6)	6.9(0.9)	25.7(10.1)	52.5(0.7)
5 MIN	25.7(1.1)	35.8(3.5)	5.2(0.4)	14.3(5.4)	19.0(0.5)
7 MIN	38.4(3.2)	42.7(4.9)	4.9(0.3)	5.6(1.5)	8.4(0.8)
15 MIN	40.0(4.3)	58.4(3.6)	0.0	0.0	0.0
140°C					
2 MIN	0.0	4.7(0.02)	3.0(0.2)	12.0(0.1)	80.3(0.2)
15 MIN	4.8(1.1)	13.1(3.9)	8.4(1.0)	11.7(1.0)	62.1(5.1)
30 MIN	16.1(4.3)	38.6(2.8)	13.4(0.2)	8.1(2.5)	23.9(4.4)
100°C					
2 MIN	0.0	0.0	0.0	1.9(1.0)	96.6(1.0)
15 MIN	0.0	0.0	0.0	9.0(0.8)	89.6(0.9)
30 MIN	0.0	0.0	0.0	20.3(0.2)	78.2(0.2)

Table 10. Products from the Reaction of Tetralin with Mo/Al_2O_3

Reaction Conditions	Weight Percent Recovered				
	t-DEC	c-DEC	1,2-DHN	NAP	TET
TETRALIN					
450°C					
15 MIN	28.4(0.1)	0.0	29.0(0.5)	2.4(0.1)	40.3(0.2)
30 MIN	39.2(0.2)	0.0	40.9(0.4)	1.9(0.4)	18.0(1.0)
60 MIN	44.1(1.4)	0.0	42.8(1.5)	2.0(0.2)	11.1(0.4)
425°C					
15 MIN	0.0	0.0	17.7(0.3)	2.2(0.2)	80.2(0.5)
30 MIN	0.8(0.2)	0.0	45.6(0.8)	3.0(0.1)	50.7(0.8)
60 MIN	35.7(0.6)	0.0	36.5(0.9)	1.6(0.3)	26.2(0.9)
380°C					
2 MIN	0.0	0.0	0.0	trace	100.0
15 MIN	2.7(0.3)	0.0	0.0	0.0	97.3(0.3)
30 MIN	3.1(0.6)	1.3(0.2)	0.0	0.7(0.5)	94.9(1.5)
60 MIN	1.2(1.4)	0.0	6.0(0.2)	0.0	92.8(1.4)

Table 11. Products from the Reaction of Tetralin with $NiMo/Al_2O_3$

Reaction Conditions	Weight Percent Recovered				
	t-DEC	c-DEC	1,2-DHN	NAP	TET
TETRALIN					
450°C					
15 MIN	30.2(0.2)	10.1(1.3)	26.5(1.9)	1.6(1.1)	31.6(0.8)
30 MIN	44.4(1.3)	10.6(0.6)	25.9(0.3)	0.9(1.1)	18.2(1.1)
60 MIN	56.8(0.5)	12.2(1.4)	28.6(0.8)	1.4(0.4)	1.0(0.1)
425°C					
15 MIN	24.0(0.8)	8.9(0.8)	24.5(0.7)	1.9(0.1)	40.7(1.5)
30 MIN	33.9(1.5)	9.1(0.7)	35.3(3.4)	1.2(0.4)	20.4(3.2)
60 MIN	43.6(1.0)	6.2(0.9)	43.9(1.1)	0.5(0.1)	5.8(0.7)
380°C					
2 MIN	3.2(1.1)	trace	0.0	0.0	96.8(1.1)
15 MIN	33.0(1.6)	12.0(0.5)	0.0	0.0	55.0(2.1)
30 MIN	56.5(1.5)	19.0(0.5)	0.0	0.0	24.5(3.5)
60 MIN	57.4(1.2)	20.7(0.5)	0.0	0.0	21.9(1.4)

Table 12. Products from the Reaction of Dihydroanthracene with Mo/Al_2O_3

Reaction Conditions	OHA	THA	ANT	DHA
DHA				
380°C				
2 MIN	0.0	22.7(1.0)	2.5(0.2)	74.8(1.0)
15 MIN	40.2(4.4)	34.5(1.0)	1.1(0.2)	24.2(3.2)
30 MIN	70.8(2.0)	21.2(1.0)	0.0	8.0(1.1)
60 MIN	76.0(0.2)	17.7(0.1)	0.0	6.3(0.1)
350°C				
15 MIN	0.0	7.6(1.8)	3.0(0.4)	89.4(1.8)
30 MIN	0.0	13.9(4.3)	3.1(0.2)	83.0(4.2)
60 MIN	10.6(6.9)	26.9(1.3)	2.2(0.2)	57.8(3.9)
300°C				
15 MIN	0.0	2.3(0.1)	1.7(0.1)	96.0(0.2)
30 MIN	0.0	4.4(1.1)	1.6(0.4)	94.0(1.4)
60 MIN	0.0	8.1(0.8)	1.5(0.1)	90.4(0.7)

Table 13. Products from the Reaction of Dihydroanthracene with $NiMo/Al_2O_3$

Reaction Conditions	PHA	OHA	THA	DHA
DHA				
380°C				
2 MIN	6.9(0.8)	0.0	6.3(1.2)	86.8(0.4)
5 MIN	12.7(0.8)	55.9(0.3)	8.8(0.6)	26.6(0.5)
15 MIN	17.5(0.5)	68.6(0.6)	12.9(0.3)	1.0(0.5)
30 MIN	64.0(2.2)	35.0(5.0)	1.0(0.1)	0.0
350°C				
15 MIN	21.3(0.4)	7.4(0.1)	2.5(0.5)	68.8(1.8)
30 MIN	30.1(1.2)	6.0(0.4)	2.4(1.0)	61.6(4.2)
60 MIN	49.9(0.4)	3.8(0.1)	2.3(0.3)	44.0(3.9)
300°C				
15 MIN	21.1(0.7)	10.1(0.3)	0.0	68.8(0.2)
30 MIN	24.8(0.7)	8.5(0.3)	0.0	66.7(1.4)
60 MIN	30.1(0.3)	7.5(0.1)	0.0	62.4(0.7)
90 MIN	34.6(0.5)	19.8(0.3)	0.0	45.6(0.9)

Table 14. Products from the Reaction of Octahydroanthracene with Mo/Al_2O_3

Reaction Conditions	Weight Percent Recovered				
	PHA	THA	DHA	ANT	OHA
OHA					
450°C					
15 MIN	16.2(0.3)	17.5(0.6)	0.0	0.0	66.3(0.8)
30 MIN	19.1(0.4)	18.9(1.1)	0.0	0.0	62.1(0.8)
60 MIN	13.6(4.6)	36.5(3.6)	0.0	11.8(1.6)	38.2(5.3)
425°C					
15 MIN	8.3(0.6)	9.7(0.1)	0.0	0.0	82.0(0.7)
30 MIN	9.3(0.7)	18.1(2.7)	0.0	0.0	72.6(2.0)
60 MIN	22.9(0.9)	12.2(1.1)	0.0	0.0	65.0(1.8)
380°C					
2 MIN	0.0	0.0	0.0	0.0	100.0
30 MIN	0.0	2.2(0.1)	0.0	0.0	97.8(0.1)
60 MIN	4.7(0.1)	2.6(0.1)	2.2(0.2)	0.0	90.5(0.2)
90 MIN	6.5(0.2)	4.9(0.2)	2.6(0.2)	0.0	86.0(0.8)

Table 15. Products from the Reaction of Octahydroanthracene with $NiMo/Al_2O_3$

Reaction Conditions	Weight Percent Recovered				
	PHA	THA	DHA	ANT	OHA
OHA					
450°C					
15 MIN	50.5(0.3)	9.4(0.1)	7.1(0.2)	3.5(0.2)	29.5(1.0)
30 MIN	63.3(1.9)	5.8(1.3)	7.0(0.5)	5.3(0.4)	18.6(1.3)
60 MIN	75.8(2.2)	3.8(0.7)	5.3(0.4)	7.3(2.2)	7.9(1.0)
425°C					
15 MIN	42.2(1.2)	8.3(0.4)	4.0(0.2)	0.0	45.5(1.7)
30 MIN	66.8(0.3)	3.9(0.9)	3.4(0.5)	0.0	25.9(1.3)
60 MIN	78.6(3.1)	2.3(0.6)	2.6(0.6)	0.0	16.5(1.8)
380°C					
2 MIN	17.2(3.2)	trace	0.0	0.0	82.8(3.2)
15 MIN	52.9(0.4)	0.0	0.0	0.0	47.1(0.4)
30 MIN	68.0(4.9)	0.0	0.0	0.0	32.0(3.7)
60 MIN	80.4(0.3)	0.0	0.0	0.0	19.6(0.3)

Table 16. Products from the Reaction of Hexahydroanthracene with Mo/Al_2O_3

Reaction Conditions	Weight Percent Recovered				
	PHA	OHA	THA	DHA	HHA
HHA					
225°C					
2 MIN	2.3(0.2)	42.8(3.3)	3.8(0.9)	1.9(0.1)	49.2(4.4)
5 MIN	7.2(0.2)	47.7(3.8)	15.6(4.4)	0.0	29.5(1.0)
15 MIN	5.8(0.2)	78.7(1.3)	14.0(2.9)	0.0	1.5(1.8)
175°C					
2 MIN	0.0	8.9(0.2)	5.9(0.2)	0.0	85.2(0.5)
15 MIN	0.0	10.2(0.3)	6.7(0.2)	0.0	83.1(0.5)
30 MIN	0.0	29.8(4.8)	8.1(0.7)	1.2(0.2)	60.9(4.5)
125°C					
2 MIN	0.0	0.5(1.7)	2.0(1.1)	0.0	97.5(2.8)
15 MIN	0.0	2.0(1.4)	2.7(0.7)	0.0	95.2(2.0)
30 MIN	0.0	12.0(0.2)	4.7(0.3)	5.95(2.5)	77.4(2.1)

Table 17. Products from the Reaction of Hexahydroanthracene with $NiMo/Al_2O_3$

Reaction Conditions	Weight Percent Recovered				
	PHA	OHA	THA	DHA	HHA
HHA					
175°C					
2 MIN	0.0	32.2(0.5)	10.0(0.3)	2.1(0.1)	55.8(0.8)
5 MIN	0.0	50.2(1.5)	26.4(0.5)	1.0(0.2)	22.4(2.1)
7 MIN	0.0	69.9(1.0)	25.3(0.8)	0.0	4.8(0.2)
140°C					
2 MIN	0.0	14.8(1.3)	10.2(0.8)	1.7(0.4)	73.3(1.7)
15 MIN	0.0	23.2(5.4)	9.2(0.4)	1.5(0.1)	66.1(5.1)
30 MIN	0.0	38.9(2.9)	7.3(0.5)	1.2(0.1)	52.6(3.2)
60 MIN	0.0	55.7(1.4)	10.2(0.5)	5.4(0.3)	28.7(1.1)
100°C					
2 MIN	0.0	8.3(0.6)	4.0(0.3)	1.3(0.1)	86.4(0.9)
15 MIN	0.0	13.9(0.6)	8.9(0.7)	1.3(0.3)	76.0(1.5)
30 MIN	0.0	17.8(0.1)	10.6(0.9)	1.6(0.04)	70.0(0.7)

Table 18. Apparent Rate Constants and Arrhenius Parameters for the Model Compound Catalytic Reactivity Studies

Reaction Conditions	Apparent Rate Constant (k)	Correlation Coefficient for Rate Constant	Arrhenius Parameters
DHA			
AMOCAT 1B			
380°C	0.04662	0.91585	E_a/R = 15,271
350°C	0.00913	0.98452	$k_o = 5.47 \times 10^8$
325°C	0.00162	0.98452	r = 0.98719
SHELL 324			
380°C	0.32024	0.99535	E_a/R = 16,005
350°C	0.01285	0.97363	$k_o = 6.31 \times 10^9$
300°C	0.00714	0.92195	r = 0.84895
HHA			
AMOCAT 1B			
225°C	0.27672	0.99744	E_a/R = 6,827
175°C	0.01403	0.93771	$k_o = 1.48 \times 105^6$
125°C	0.00796	0.93897	r = 0.90529
SHELL 324			
175°C	0.41279	0.97223	E_a/R = 8,499
140°C	0.01865	0.97747	$k_o = 5.89 \times 10^7$
100°C	0.01036	0.92164	r = 0.97333
OHA			
AMOCAT 1B			
450°C	0.01507	0.97803	E_a/R = 14,590
425°C	0.00687	0.95319	$k_o = 8.57 \times 10^6$
380°C	0.00172	0.98408	r = 0.99944
SHELL 324			
450°C	0.03969	0.96163	E_a/R = 2510
425°C	0.02893	0.95466	$k_o = 1.18 \times 10^0$
380°C	0.02633	0.96853	r = 0.88137
ISO			
AMOCAT 1B			
225°C	0.56506	0.99341	E_a/R = 9,516
175°C	0.04508	0.97607	$k_o = 1.20 \times 10^8$
125°C	0.00430	0.97135	r = 0.99635
SHELL 324			
175°C	0.35181	0.99877	E_a/R = 8,370
140°C	0.04430	0.97346	$k_o = 3.82 \times 10^7$
100°C	0.00783	0.99431	r = 0.98996
TET			
AMOCAT 1B			
450°C	0.03575	0.95051	E_a/R = 23,311
425°C	0.02299	0.99546	$k_o = 4.78 \times 10^{12}$
380°C	0.00130	0.97524	r = 0.97774
SHELL 324			
450°C	0.07561	0.98836	E_a/R = 6,702
425°C	0.04664	0.99646	$k_o = 7.56 \times 10^2$
380°C	0.02716	0.92257	r = 0.98773

E_a = activation energy R = Universal gas constant
k_o = frequency factor r = correlation efficient

FIGURE 1.
PLOT OF GIBBS FREE ENERGY vs TEMPERATURE.
NITROGEN ATMOSPHERE

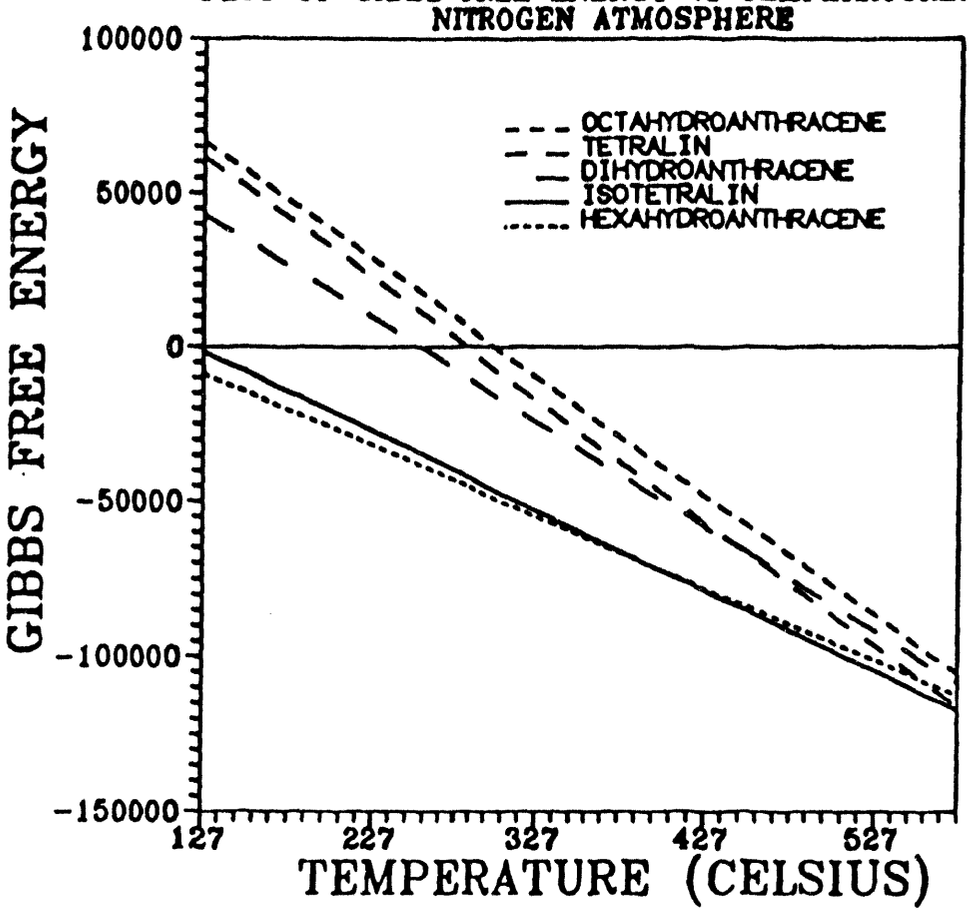

FIGURE 2.
PLOT OF GIBBS FREE ENERGY vs TEMPERATURE.
HYDROGEN ATMOSPHERE

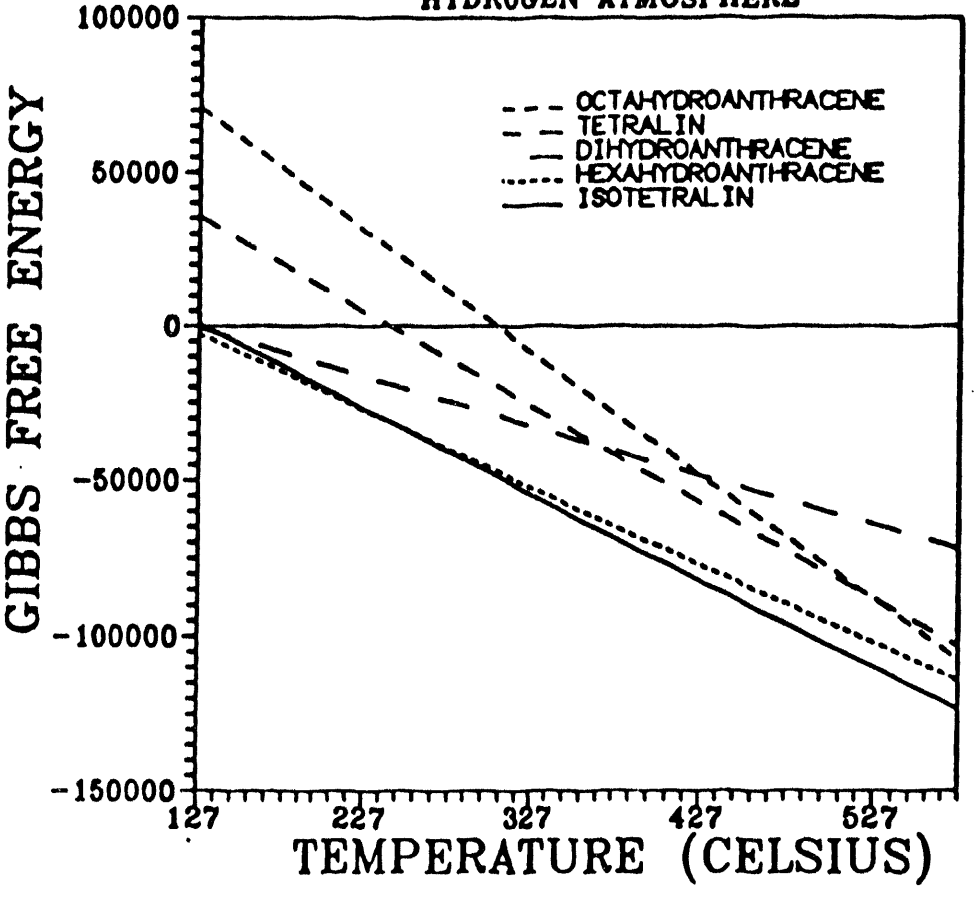

FIGURE 3.
PLOT OF GIBBS FREE ENERGY vs TEMPERATURE.
AMOCAT 1B

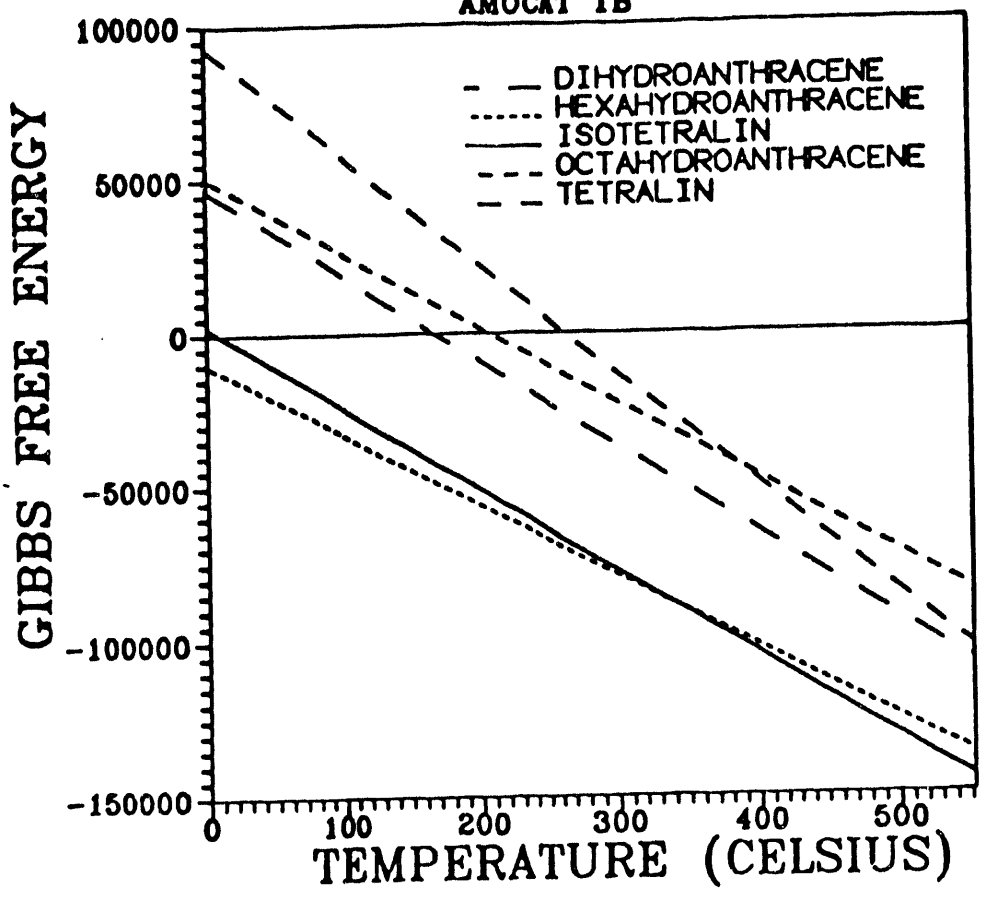

FIGURE 4.
PLOT OF GIBBS FREE ENERGY vs TEMPERATURE.
SHELL 324

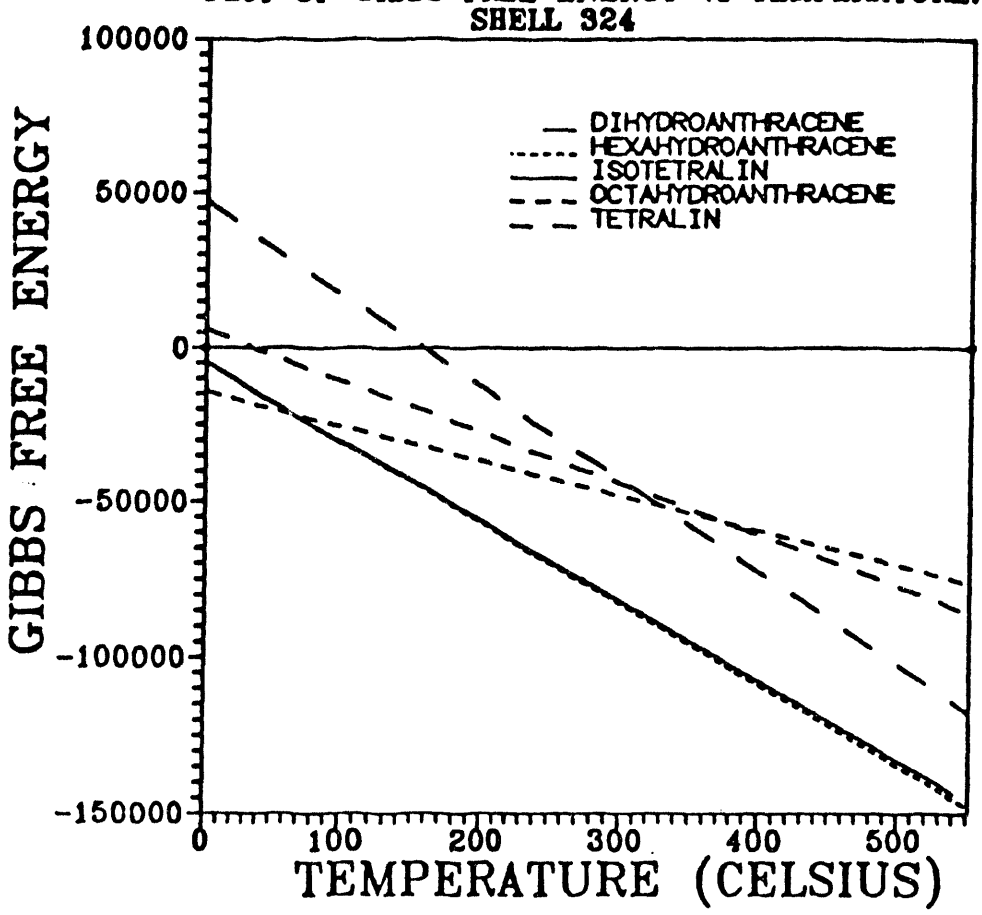

DATE FILMED

4/6/94

END